https://doi.org/10.2352/ISSN.2470-1173.2021.17.AVM-173

End-to-End Imaging System Optimization for Computer Vision in Driving Automation

Korbinian Weikl[1,2], Damien Schroeder[2], Daniel Blau[1], Zhenyi Liu[3], and Walter Stechele[1]
[1]Department of Electrical and Computer Engineering, Technical University of Munich, Munich, Germany
[2]Automated Driving, BMW Group, Munich, Germany
[3]State Key Laboratory of Automotive Simulation and Control, Jilin University, Changchun, China

Abstract

Full driving automation imposes to date unmet performance requirements on camera and computer vision systems, in order to replace the visual system of a human driver in any conditions. So far, the individual components of an automotive camera have mostly been optimized independently, or without taking into account the effect on the computer vision applications. We propose an end-to-end optimization of the imaging system in software, from generation of radiometric input data over physically based camera component models to the output of a computer vision system. Specifically, we present an optimization framework which extends the ISETCam and ISET3d toolboxes to create synthetic spectral data of high dynamic range, and which models a state-of-the-art automotive camera in more detail. It includes a state-of-the-art object detection system as benchmark application. We highlight in which way the framework approximates the physical image formation process. As a result, we provide guidelines for optimization experiments involving modification of the model parameters, and show how these apply to a first experiment on high dynamic range imaging.

Introduction

Despite continued effort invested into driving automation by the research community as well as the industry, there still is no system available that pushes for the highest level of driving automation on public roads. To reach full driving automation (level 5, as defined in [1]) at the reliability expected by customers and the general public, advanced sensor setups will be required: Unconditional operation of the automated system requires shifting the sensor setup's operational design domain (ODD) limits, and fail-safe operation requires redundancy within the sensor setup.

The ODD limits as well as the physical operating principles that can be exploited for redundant sensing are always defined by the application. In the context of cameras as sensors and computer vision (CV) as their application in driving automation, an important ODD limit is a low-light threshold for reliable performance. A redundancy that can be used is object appearance in multiple spectral bands. Neither a shift of the low-light threshold (ultra low-light imaging) nor imaging outside the visible spectrum (spectrally extended imaging) are typical camera design objectives focused on human vision applications. These examples make clear that the specialization of cameras for driving automation needs to be guided by optimization for the CV systems that process the camera output data.

This specialization has several implications on the camera development and design process. Firstly, there are only few quality metrics available, for the overall imaging pipeline as well as camera component interfaces, that have proven to be descriptive of quality for CV applications. The IEEE P2020 working group is currently working towards a first standard to define such metrics [2]. At the same time, setting full driving automation as the goal of camera design imposes very high and so far unmet performance requirements. The best way to manage these challenges is to pursue an end-to-end optimization of the imaging system, which allows use of performance metrics of the target application for the objective function and to reach a globally optimal solution. Equally, state-of-the art CV systems are based on machine learning (ML) and hence require a data-driven development process. In each iteration of a camera optimization for CV, the tested camera must produce a large enough dataset to train and test the CV. At the same time, as indicated by the example of spectrally extended imaging, redefining imaging systems as sensors for an automated system instead of as devices that mimic human vision opens a very large design space. The best way to cope with this design complexity is to use a simulation system that scales well. This has also been called "soft prototyping" [3]. In this work, we present a camera optimization framework that accounts for these implications. It integrates a large scale data generation, detailed automotive camera model and benchmark CV system as end-to-end pipeline in a simulation environment.

The framework is based on the ISETCam [4, 5] camera simulation toolbox and ISET3d [6] toolbox for synthetic scene generation. These toolboxes have been used in the context of driving automation before [7, 8, 3, 9], implementing an open source framework for automotive camera simulation which we use as template for our framework. The recent survey by Tsirikoglou *et al.* [10] gives an extensive overview of similar approaches that use synthetic data for ML applications. The survey also puts forward two of the main arguments for using synthetic data for ML: First, it offers the flexibility to generate datasets that are not only large, but also follow a given data distribution, i.e. dataset statistics such as class distribution. Second, training and testing on synthetic data allows a detailed performance analysis for benchmarking, using comprehensive scene metadata. Further approaches to camera optimization for CV focus on ISP optimization [11, 12, 13].

We present several extensions to the existing camera simulation and optimization framework required to more accurately model automotive imaging systems. The main contributions are methods for camera placement as part of an ego vehicle within scene generation, and a toolset for simulation of generic high dynamic range (HDR) camera models. We compare the framework's data flow to the physical image formation process and highlight

benefits, but also limitations of our framework's approach. As the primary result of this comparison, we give guidelines for systematic end-to-end optimization using our framework: We identify the paths for iterative optimization involving modification of the model parameters. We also demonstrate how these apply to a first experiment on HDR imaging.

Optimization framework

The framework we propose uses the same building blocks as its basis presented in [7, 8, 3]: A module for large scale synthetic scene generation; physically based camera simulation consisting, fundamentally, of sensor and image signal processor (ISP) models; and a ML based CV model as benchmark application. The camera lens model is included within synthetic scene generation. Fig. 1 gives an overview of the framework's building blocks.

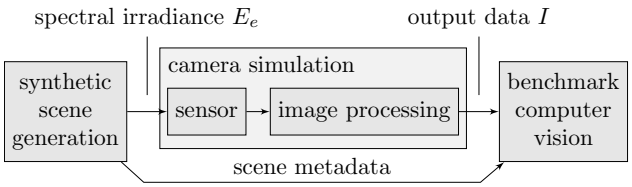

Figure 1. *Framework overview: End-to-end optimization is enabled by embedding the camera simulation between modules for synthetic scene generation and benchmark computer vision.*

Physical image formation process

In order for the optimization results to be transferable to hardware implementation, we define as aim of our camera simulation to approximate the physical image formation process with respect to all its elements that affect the camera output data. The physical image formation processes can be depicted as the pipeline in Fig. 2. It is described in more details in [5].

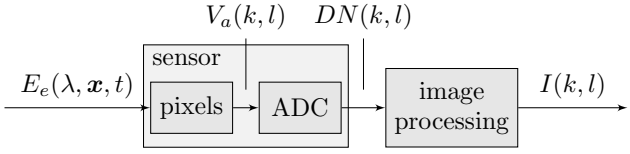

Figure 2. *The physical image formation process as data pipeline.*

Input to the process is the spectral irradiance $E_e(\lambda,\boldsymbol{x},t)$ of wavelength λ that hits the sensor surface at location $\boldsymbol{x}$ and time t. Within the sensor's pixel circuitry, this radiometric quantity is translated to an analog voltage $V_a(k,l)$ at pixel position (k,l). The voltage signal is quantized to a digital number representation $DN(k,l)$, which we also call the raw sensor data. Using image processing, the raw sensor data can be transformed to a data format that can be interpreted as a natural image $I(k,l)$ by human vision. Image processing transformations can also be used as preprocessing steps for CV applications. We thus more generally refer to $I(k,l)$ as camera output data.

Not considering noise sources, the translation from irradiance to noise-free analog voltage $\widetilde{V}_a$ can be formalized as

$$\widetilde{V}_a(k,l) = g_c \iiint_D H(\lambda,\boldsymbol{x}) E_e(\lambda,\boldsymbol{x},t)\, d\lambda\, d\boldsymbol{x}\, dt, \qquad (1)$$

where we denote $D = \{(\lambda,\boldsymbol{x},t) | \lambda \in \Lambda, \boldsymbol{x} \in S_p, t_0 < t < t_1\}$ the domain defined by the sensor's sensitive spectral range Λ, the effective pixel surface S_p, and the exposure start time and end time t_0 and t_1; $H(\lambda,\boldsymbol{x})$ the sensor quantum efficiency, i.e. the effective spectral charge generation efficiency defined by global filters, color filter array (CFA), and pixel quantum efficiency; and g_c the conversion gain.

Importantly for the adaptation in our framework, eq. (1) shows that the input irradiance is integrated in the spectral, spatial, and temporal dimensions within the pixel: The pixel accumulates charge generated by any photons of a wavelength within Λ, that hit the pixel surface during the exposure time interval. The pixel circuit converts this charge to a voltage, at a factor defined by the conversion gain.

Synthetic scene data

As the first module of the framework, the synthetic scene generation produces the irradiance data that is required to stimulate the physically based camera simulation. Its core is the physically based rendering module based on [14, 15], shown in Fig. 3. It simulates the physical light transport through a scene modeled by the spectral radiance $L_e(\lambda,\boldsymbol{\omega}_o,\boldsymbol{x},t)$ that light sources distribute from locations $\boldsymbol{x}$ into direction $\boldsymbol{\omega}_o$, and the bidirectional scattering distribution functions (BSDFs) of the objects in the scene.

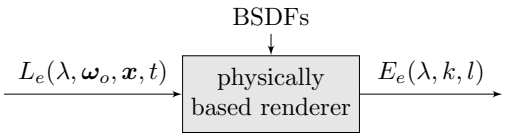

Figure 3. *The core of synthetic scene generation: Physically based rendering based on [14, 15] as source of spectral irradiance data.*

The rendering implicitly includes a spatial and temporal integration, since sensor surface grid as well as object positions and their dynamic transformations during the exposure time interval have to be defined for the light transport simulation by ray tracing algorithms. An additional constraint for the ray tracing is the grid of wavelengths λ on which it is evaluated. Hence, other than in the physical image formation process, the output spectral irradiance $E_e(\lambda,k,l)$ is defined for fixed pixel surfaces at locations (k,l), a fixed exposure time as well as a fixed spectral grid. We also refer to it as optical image (OI), using ISETCam naming.

ISET3d includes a large set of tools to automatically generate the description files of realistic automotive scenes that are input to the renderer. We extend these tools in our framework, first, to include a more detailed model of the camera mount. We replace one of the car objects in the scene by our ego vehicle model and position the camera at the ego vehicle's camera mount behind the windshield. This is the typical automotive front camera position to date. An RGB visualization of an examplary OI, of a scene including our ego vehicle model, is shown in Fig. 4.
Using this extension, the ego vehicle follows ISET3d's realistic traffic flows and the camera's optical path is completed by stray light cover and windshield. As future work, we plan to refine and validate the windshield geometry and material models, in order to realistically reproduce its impact on camera performance.

We extend the tools, second, to generate an arbitrary number of scene descriptions from the same scene configuration, i.e. de-

Figure 4. *OI of a scene including our ego vehicle model. A part of the stray light cover as well as some distortions caused by the windshield are visible in the lower periphery of the image.*

scriptions which use the same lighting, object and material composition, but differ in their $[t_0, t_1]$ exposure timing. We determine the correct positions and dynamic transformations of camera and dynamic objects for each exposure, interpolating object position and motion information from the scene's traffic flow. As will be shown in the following, we generate the exposure timing information in the camera simulation model. This extension is an important prerequisite for HDR imaging simulation, since it allows to realistically produce HDR camera output data including dynamic image artifacts.

Third, we extend the abilities to use ISET3d's scene configuration as an abstract model of the scene, allowing us to tailor the scene statistics. We create criteria for ego vehicle placement, e.g. such that the ego vehicle faces a portion of the scene populated by other objects. We modify object dynamics based on the objects' class membership to alter the speed limits of all traffic participants, and rotate the skymap for challenging natural lighting conditions such as glare by direct sunlight.

Physically based camera simulation

The core module of our framework is the physically based camera simulation. It includes sensor and image processing models as shown in Fig. 1. Within the sensor simulation, the noise-free analog voltage signal is calculated as

$$\widetilde{V}_a(k,l) = g_c \cdot A_p \cdot t_{exp} \int_\Lambda H(\lambda,k,l) E_e(\lambda,k,l)\, d\lambda. \tag{2}$$

Due to the implicit spatial and temporal irradiance integration within scene generation, the effective pixel surface area A_p and exposure time $t_{exp} = t_1 - t_0$ become simple factors compared to eq. (1).

Of particular interest in this equation is the spectral integration. In photometry, the amount of light incident on a surface as seen by a human observer is measured by the illuminance

$$E_v = \int_{\Lambda_v} V(\lambda) E_e(\lambda)\, d\lambda, \tag{3}$$

where $V(\lambda)$ denotes the "CIE spectral luminous efficiency function for photopic vision" [16] defined over the visible spectrum Λ_v. Equivalently, as a measure of the amount of light incident on the sensor surface, we can use the current density j generated in the pixel's photodiode,

$$j(k,l) = \int_\Lambda H(\lambda,k,l) E_e(\lambda,k,l)\, d\lambda. \tag{4}$$

It directly links to the sensor's analog output dynamic range DR_a and SNR by

$$V_a(j) = \widetilde{V}_a(j) + V_n(j) = g_c \cdot A_p \cdot t_{exp} \cdot j + V_n(j), \tag{5}$$

$$DR_a = \frac{V_{a,max}}{V_{a,min}} = \frac{V_a(j_{max})}{V_a(j_{min})}, \quad SNR = \frac{\widetilde{V}_a(j)}{V_n(j)}, \tag{6}$$

where V_n denotes the noise component of V_a summarized as additive term and j_{max} marks output saturation. j_{min} is commonly defined by $SNR_{dB} = 0\,dB \Leftrightarrow SNR = 1$. As reference for dynamic range (DR) definitions and contributions to $V_n(j)$, see [17]. Consequently, we can can define an input DR as

$$DR_j = \frac{j_{max}}{j_{min}}. \tag{7}$$

We extend the camera simulation by a toolset for HDR imaging, first presented in [18]. Traditionally, HDR imaging refers to DRs of photometric input quantities. In contrast, our toolset is based on DR_j. It is not subjective to human vision, and therefore does not introduce a bias when used in the context of camera optimization for CV.

Since j depends on the pixel position within the CFA pattern, we use the current density of a clear pixel,

$$j_c(k,l) = \int_\Lambda H_c(\lambda) E_e(\lambda,k,l)\, d\lambda, \tag{8}$$

to calculate the histogram and DR of an OI. $H_c(\lambda)$ denotes the sensor quantum efficiency of a clear pixel, i.e. a pixel without CFA impact. As single dynamic range (SDR) sensor, we use the SDR model of a state-of-the-art automotive 8 Mpx imager with RYYCy CFA presented in [19]. Our HDR camera models are based on the SDR model, and suitable as template for any HDR imaging concepts in which the final image is constructed by combining a set of separate exposures of the same scene. These exposures can correspond to very different HDR imaging approaches. Our models include temporally sequential exposures of different duration (multi-exposure), temporally parallel exposure of different photodiodes (split-pixel), exposure readout by multiple pixel circuit configurations (dual conversion gain) and temporally shifted exposures caused by pixel resets (multiple slopes) [18]. The common property of these exposures is that they allow an HDR camera to concurrently operate at several sensitivity levels. From this starting point, our HDR toolset enables to

- generate a histogram of an OI based on j_c, and the OI DR which we constrain by the percentage of outliers. As outliers we denote a small number of pixels that we neglect at both DR ends for a more robust DR estimation.
- generate the SNR curve, i.e. SNR(j) for $j_{min} < j < j_{max}$ for our SDR model.
- generate an optimized HDR SNR curve for a given HDR camera model, for a target DR and / or a minimum SNR at the transition point between exposures. This sets the ratios of the exposures' sensitivities for this camera model.
- for an HDR camera model with known sensitivity ratios and an OI histogram of a scene rendered for a frame's maximum exposure time $t_{exp,max}$, perform a temporal auto-exposure. The auto-exposure goal is to align the upper DR limits of OI and camera, i.e. only allow the outliers to saturate. The

overall exposure time is constrained by $t_{exp,max}$. This determines the exposure settings for the given camera and scene.
- regenerate the given synthetic scene for each exposure of the HDR camera.
- generate the HDR camera output data, re-combining the sensor responses to the individual exposures.

Fig. 5 shows the OI of an exemplary scene, as well as auto-exposure results of two camera models for this scene. The SDRCam model implements our SDR sensor model, the MEDCGCam model comprises four temporally sequential exposures and dual conversion gain to further increase the maximum sensitivity of the most sensitive exposure. Fig. 6 shows alternative auto-exposure results for a tighter bound on the OI DR. Fig. 7 shows the resulting camera output data for the scene and auto-exposures shown in Fig. 5, with detections of the experiment described in the results section. The lower DR of the SDR camera results in missing details and visible noise in the scene's low-light regions.

For exposure recombination, we use the most sensitive exposure as starting point and replace saturated pixels using less sensitive exposures. We use a simple ISP model that can process raw sensor data from sensors with RYYCy CFA, but which is visibly limited in terms of color reproduction. The ISP model does also not include data pre-processing for CV such as region-of-interest cropping. More advanced models for ISP and recombination, as well as auto-exposure including sensor gain settings remain future work.

Benchmark computer vision

The concluding module of our end-to-end optimization framework is the CV model that serves as benchmark application, i.e. the output performance metrics of which we use as objective functions for the camera design. The CV module operates on camera output data I and additionally receives scene metadata from the scene generation module as shown in Fig. 1. The metadata is required for CV model training (supervised learning) and output metric calculation during normal operation (inference). We choose object detection as first benchmark application, given its importance for detection of traffic signs and traffic lights, other traffic participants, obstacles and other traffic-related objects in driving automation. The CV model we implement is CenterNet with DLA-34 backbone [20]. It can be used for 2D and 3D object detection.

Following KITTI notation [21], we extract bounding box labels from ISET3d's scene metadata. The available metadata includes object class, depth, and world coordinates for each pixel of a rendered scene and hence is sufficient for 2D and 3D bounding boxes. As future work we plan to extend the scene metadata generation beyond pixel-level annotations, in order to be able to include e.g. object occlusion, truncation and orientation.

Results

The primary result of this work is a set of guidelines that determine how the proposed framework can be used for end-to-end optimization of imaging systems.

End-to-end optimization diagram

Within the framework, there are three main interfaces at which pre-computed data can be reused in optimization iterations,

(a) OI of a scene with large DR caused by sun glare and deep shadows. Compressed and transformed to RGB for visualization.

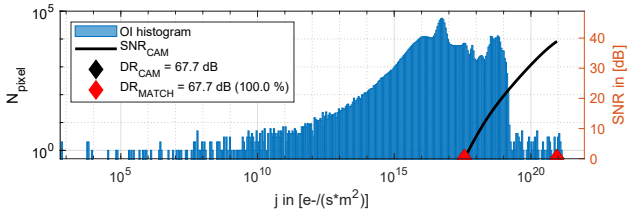

(b) SDRCam SNR curve for OI in (a) and 0.001 % outliers

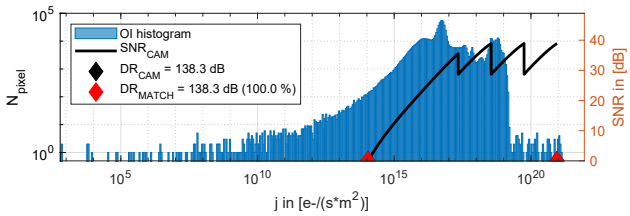

(c) MEDCGCam SNR curve for OI in (a) and 0.001 % outliers

Figure 5. *Proposed HDR toolset: Visualization of an auto-exposure of our SDR model and a derived HDR model for an examplary OI. The cameras' SNR curves SNR_{CAM} overlaid the OI histogram visualize to what extent the camera models cover the scene's DR. This is also expressed as DR_{MATCH}, i.e. the overlap of the camera's dynamic range DR_{CAM} with the OI's DR. N_{pixel} denotes the number of pixels in the histogram bins.*

given only parameters of following modules are modified. These are the synthetic scene irradiance data E_e, the raw sensor data DN and the camera output data in image format I. The latter is complemented by the corresponding scene metadata. It is important to use these interfaces in order to cope with the large computational effort associated with physically based rendering and physically based camera simulation, especially in the context of large dataset generation for CV training and testing.

At the same time, it is inevitable that for parameter modifications that affect the data at these interfaces, the data must be recomputed. This is especially noteworthy since as we have described in the previous section, the framework's data pipeline differs from the physical image formation process. These differences can be summed up as follows:

- All camera components that affect the camera's optical path, particularly the camera lens and camera mount, are modeled within the synthetic scene generation.
- All parameters that modify the simulation's spectral or spatial grid or its temporal boundaries, affect synthetic scene

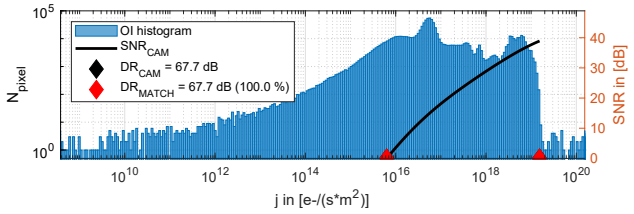

(a) SDRCam SNR curve for OI in Fig. 5a and 0.01 % outliers

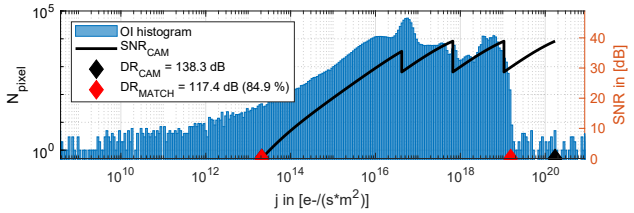

(b) MEDCGCam SNR curve for OI in Fig. 5a and 0.01 % outliers

Figure 6. *Alternative auto-exposure for the scene and camera models in Fig. 5, allowing more outliers to create a tighter bound for the OI DR. This way, SDRCam covers a part of the OI DR that contains a larger fraction of the image pixels. The MEDCGCam auto-exposure is limited by* $t_{exp,max}$.

generation.

Fig. 8 summarizes the resulting paths for iterative imaging system optimization.

First optimization experiment

As first experiment for camera optimization, we compare the two camera models SDRCam and MEDCGCam with their DR and SNR characteristics as shown in Fig. 5. Following Fig. 8, from a set of scene configurations we generate separate synthetic scene datasets for each model. We generate the camera output data as shows in Fig. 7 and 2D bounding box labeling data for the objects of car and pedestrian classes. In this first experiment, we directly observe the CV model performance, using a version of our model that is pre-trained for the KITTI 3D object detection dataset [21] and the 2D (image plane) bounding box component of the detections as output. As the detection overlays in Fig. 7 show for that exemplary scene, the extended DR of the MEDCGCam model directly enables detection of vehicles which for the SDRCam model are covered by noise in the low-light shadows. This is an extreme example due to the auto-exposure settings shown in Fig. 5, which especially for the SDRCam lead to very limited low-light performance. A quantitative evaluation based on large enough HDR datasets that allow CV training remain future work.

Conclusion

In this work, we present a framework for end-to-end imaging system optimization in the context of driving automation, i.e. a framework suitable for optimization of the complete camera system used as sensor for a CV application. We introduce the building blocks of the framework, focusing on our extensions including a toolset for detailed simulation of HDR imaging and methods for camera placement as part of an ego vehicle. We also compare the framework's data pipeline to the physical image formation process. This comparison results in guidelines for usage of the framework in camera optimization experiments. Finally, we include results for a first experiment on HDR imaging which shows

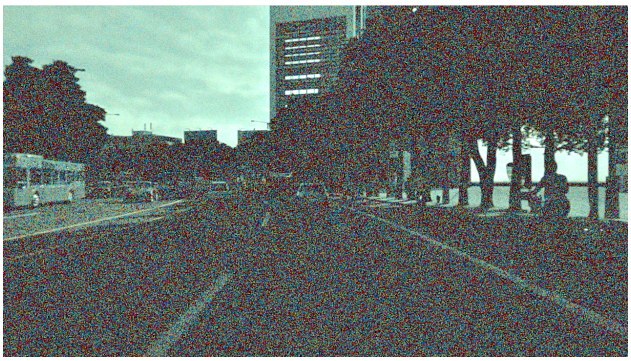

(a) SDRCam

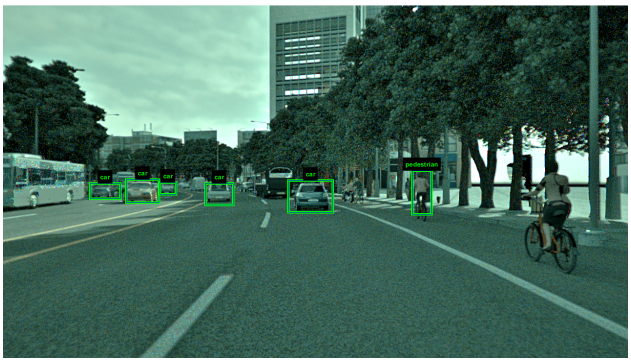

(b) MEDCGCam

Figure 7. *HDR camera simulation: Output data of SDRCam and MEDCGCam for scene and auto-exposures shown in Fig. 5, and overlaid detections of a first experiment using a pre-trained CV model.*

that the camera output data depends on the camera's DR both in terms of visual quality and CV performance as expected.

As future work, we want to use the presented framework for quantitative evaluation and optimization of the camera's HDR concept, its spectral range and its front camera mount. We also want to extend the camera simulation by more advanced models for image signal processing and pre-processing for CV, and the synthetic scene generation for extended data distribution control and scene metadata.

References

[1] "Taxonomy and Definitions for Terms Related to Driving Automation Systems for On-Road Motor Vehicles," SAE International, Warrendale, PA, USA, Recommended Practice J3016, Jun. 2018.

[2] "IEEE P2020 Automotive Imaging," IEEE, New York, USA, White Paper, Aug. 2018. [Online]. Available: https://ieeexplore.ieee.org/servlet/opac?punumber=8439100

[3] Z. Liu, T. Lian, J. Farrell, and B. Wandell, "Soft Prototyping Camera Designs for Car Detection Based on a Convolutional Neural Network," in *Proc. ICCV*, 2019.

[4] Stanford Center for Image Systems Engineering, "ISETCam," 2020. [Online]. Available: https://github.com/ISET/isetcam

[5] J. E. Farrell, P. B. Catrysse, and B. A. Wandell, "Digital camera simulation," *Applied optics*, vol. 51, no. 4, pp. A80–A90, 2012.

[6] Stanford Center for Image Systems Engineering, "ISET3d," 2020. [Online]. Available: https://github.com/ISET/iset3d

[7] H. Blasinski, J. Farrell, T. Lian, Z. Liu, and B. Wandell, "Optimiz-

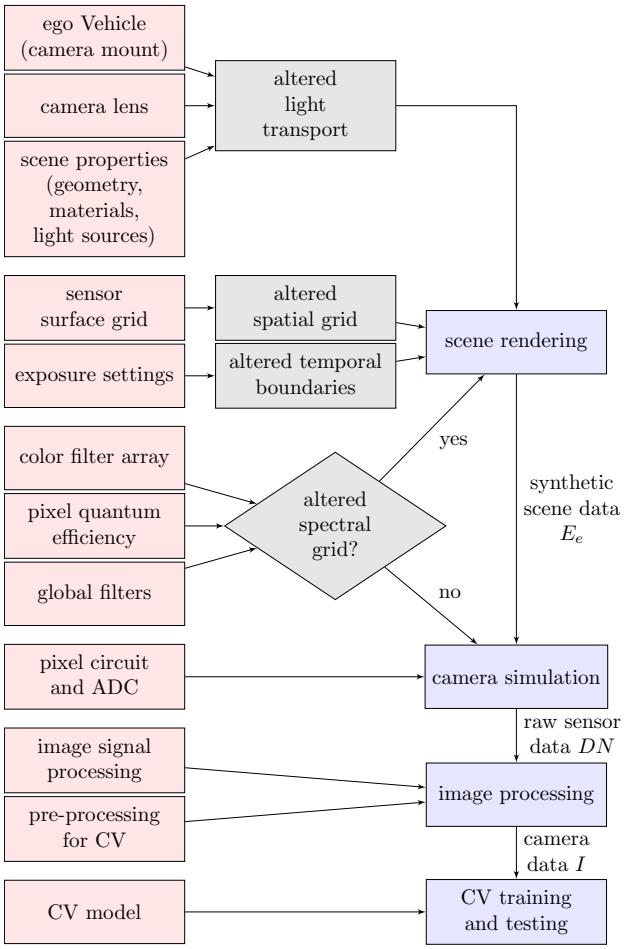

Figure 8. *Opimization diagram: Effects of parameter modification on iterative optimization paths. Model parameters are shown in red, intermediate effects of parameter modifications in grey and effects for framework building blocks in blue.*

ing Image Acquisition Systems for Autonomous Driving," in *Proc. Electronic Imaging*, 2018, pp. 161-1–161-7.

[8] Z. Liu, M. Shen, J. Zhang, S. Liu, H. Blasinski, T. Lian, and B. Wandell, "A system for generating complex physically accurate sensor images for automotive applications," in *Proc. Electronic Imaging*, 2019, pp. 53-1–53-6.

[9] Z. Liu, T. Lian, J. Farrell, and B. A. Wandell, "Neural Network Generalization: The Impact of Camera Parameters," *IEEE Access*, vol. 8, pp. 10 443–10 454, 2020.

[10] A. Tsirikoglou, G. Eilertsen, and J. Unger, "A Survey of Image Synthesis Methods for Visual Machine Learning," *Computer Graphics Forum*, vol. 39, no. 6, pp. 426–451, 2020.

[11] A. Mosleh, A. Sharma, E. Onzon, F. Mannan, N. Robidoux, and F. Heide, "Hardware-in-the-Loop End-to-End Optimization of Camera Image Processing Pipelines," in *Proc. CVPR*, Jun. 2020.

[12] E. Tseng, F. Yu, Y. Yang, F. Mannan, K. S. Arnaud, D. Nowrouzezahrai, J.-F. Lalonde, and F. Heide, "Hyperparameter Optimization in Black-box Image Processing using Differentiable Proxies," *ACM Transactions on Graphics (TOG)*, vol. 38, no. 4, Jul. 2019.

[13] L. Yahiaoui, J. Horgan, B. Deegan, S. Yogamani, C. Hughes, and P. Denny, "Overview and Empirical Analysis of ISP Parameter Tuning for Visual Perception in Autonomous Driving," *Journal of Imaging*, vol. 5, no. 10, 2019.

[14] M. Pharr, "pbrt-v3," 2020. [Online]. Available: https://github.com/mmp/pbrt-v3

[15] M. Pharr, W. Jakob, and G. Humphreys, *Physically Based Rendering*, 3rd ed. Boston, MA, USA: Morgan Kaufmann, 2016.

[16] E. Allen and S. Triantaphillidou, *The manual of photography*, 10th ed. Abingdon, U.K. and Burlington, MA, USA: Focal Press, 2011.

[17] A. Darmont, *High Dynamic Range Imaging: Sensors and Architectures*, 2nd ed. Bellingham, WA, USA: SPIE Press, 2019.

[18] D. Blau, "Comparative Evaluation of High Dynamic Range Imaging in Automotive Applications," Master's thesis, Technical University of Munich, Dec. 2020.

[19] K. Weikl, D. Schroeder, and W. Stechele, "Optimization of automotive color filter arrays for traffic light color separation," in *Proc. CIC28*, 2020, pp. 288–292.

[20] X. Zhou, D. Wang, and P. Krähenbühl, "Objects as Points," Apr. 2019, arXiv:1904.07850 [cs.CV].

[21] A. Geiger, P. Lenz, and R. Urtasun, "Are we ready for Autonomous Driving? The KITTI Vision Benchmark Suite," in *Proc. CVPR*, 2012.

Author Biography

Korbinian Weikl received his B.Sc. from the Hamburg University of Technology in 2014 and M.Sc. from the Technical University of Munich (TUM) in 2017. In 2017 he joined Rohde & Schwarz GmbH & Co. KG as development engineer for signal processing. Since 2019, he has been working as doctoral researcher affiliated with BMW Group and supervised by Prof. Dr.-Ing. Walter Stechele of TUM. His research focusses on imaging technologies for full driving automation.

Damien Schroeder received the Dipl.-Ing. degree in electrical engineering and information technology from the Technical University of Munich (TUM), Germany and the Diploma degree from Supélec, France. He joined the Chair of Media Technology at TUM in 2012, from which he received the Dr.-Ing. degree in 2017. Since 2017, he is a project manager for camera systems for automated driving with the BMW group. His research interests include video coding and camera technology.

Daniel Blau received his B.Eng. from the Nuremberg Institute of Technology in 2017 and M.Sc. from the Technical University of Munich (TUM) in 2021. In 2017, he joined vhf elektronik GmbH as development engineer for electronic and imaging systems. For his master's thesis on HDR imaging, he has been affiliated with BMW Group and supervised by Prof. Dr.-Ing. Walter Stechele of TUM.

Zhenyi Liu received his MS in Electrical Engineering at Ulsan National Institute of Science and Technology, UNIST (2015), Korea. He is currently a PhD candidate in Automotive Engineering at Jilin University, China (2016-present). Zhenyi was a Visiting Student Researcher at Stanford University (2017-2019). His research interests focus on machine perception systems for autonomous vehicles such as cameras and lidar.

Walter Stechele received the Dipl.-Ing. and Dr.-Ing. degrees in electrical engineering from the Technical University of Munich, Germany, in 1983 and 1988, respectively. In 1990 he joined Kontron Elektronik GmbH, a German electronic company, where he was responsible for the ASIC and PCB design department. Since 1993 he has been Academic Director at the Technical University of Munich. His interests include visual computing and robotic vision, with focus on Multi Processor System-on-Chip (MPSoC).

JOIN US AT THE NEXT EI!

IS&T International Symposium on

Electronic Imaging

SCIENCE AND TECHNOLOGY

Imaging across applications . . . Where industry and academia meet!

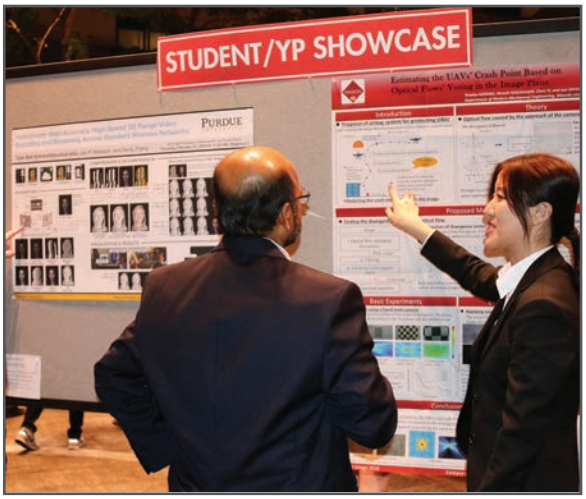

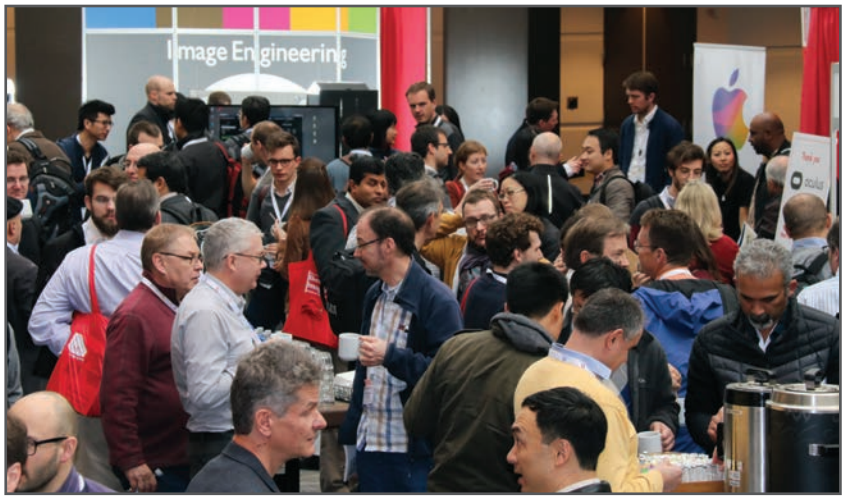

• SHORT COURSES • EXHIBITS • DEMONSTRATION SESSION • PLENARY TALKS •
• INTERACTIVE PAPER SESSION • SPECIAL EVENTS • TECHNICAL SESSIONS •

www.electronicimaging.org

IS&T
imaging.org